Desalination and Water Treatment
www.deswater.com
doi: 10.1080/19443994.2014.912593

54 (2015) 966–972
April

Taylor & Francis
Taylor & Francis Group

Modeling fouling of hollow fiber membrane using response surface methodology

Yoon-Jin Kim, Jungwoo Jung, Sangho Lee*, Jinsik Sohn

School of Civil and Environmental Engineering, Kookmin University, Jeongneung-Dong, Seongbuk-Gu, Seoul 136-702, Republic of Korea, Tel. +82 2 910 5060; Fax: +82 2 910 8597; emails: kyj_0206@hanmail.net (Y.-J. Kim), sawoo21@hanmail.net (J. Jung), jinsiksohn@gmail.com (J. Sohn); Tel. +82 2 910 4529; Fax: +82 2 910 4939; email: sanghlee@kookmin.ac.kr (S. Lee)

Received 24 January 2014; Accepted 29 March 2014

ABSTRACT

Hollow fiber membranes have been widely employed for potable water treatment, wastewater treatment and reclamation, and desalination pretreatment. They have advantages such as small footprint, ease of operation, and high removal of particles and pathogens. Nevertheless, membrane fouling is one of the most serious issues in operating hollow fiber membrane systems. Although there have been numerous researches for understanding and forecasting fouling, it is still challenging to predict fouling based on explicit mathematical models. A more practical approach is to apply statistical models, which allows more accurate fouling prediction. In this context, this study attempts the development of a statistical model to analyze fouling of hollow fiber membranes. A response surface experimental design was used to optimize and investigate the influence of process variables such as foulant types (kaolin, colloidal silica, NOM, and alginate), foulant concentration, and imposed flux on the fouling rate. The results obtained from the experiments were evaluated by multiple regression analysis method and empirical relationship between the response and independent variables. Empirical models were developed to understand the interactive correlation between the responses and process variables.

Keywords: Response surface methodology (RSM); Design of experiment (DOE); Statistical model; Hollow fiber; Membrane fouling

1. Introduction

Membrane filtration, including microfiltration (MF) or ultrafiltration (UF), is gaining popularity as a feasible option for advanced water and wastewater treatment [1,2]. The use of MF/UF has been studied by researchers since the mid-1990s and cost reduction in these technologies in a decade led to the installation of MF/UF plants [3,4]. MF/UF systems typically utilize hollow fiber modules. A major advantage of hollow fiber membrane modules over other configurations of membranes is the high membrane surface area to footprint ratio achieved by low aspect ratio (diameter-to-length ratio) of fibers. Moreover, they provide

*Corresponding author.

Presented at the 6th International Conference on the "Challenges in Environmental Science and Engineering" (CESE-2013), 29 October–2 November 2013, Daegu, Korea

cost-effective methods of removing particles and pathogenic micro-organisms from treated water [5,6].

Unfortunately, membrane fouling is one of the most serious issues in hollow fiber MF/UF systems [7,8]. The problem makes membrane difficult to control and predict. Fouling behavior is caused by various factors, including membrane surface properties, operating flux, the nature of the particle or dissolved foulants, and feed water properties [9,10]. Although there have been numerous researches for understanding and forecasting fouling, it is still challenging to predict fouling based on explicit mathematical models [11]. A more practical approach is to apply statistical models, which allows more accurate fouling prediction.

The objective of the study is to analyze fouling of hollow fiber membranes based on response surface methodology (RSM). RSM is an effective statistical tool to solve multi-variable problems, analyze the interactions among factors, and optimize one or several responses in which multiple variables may influence the outputs based on the central composite design (CCD). RSM is mainly advantageous in the less experimental trials needed to evaluate multiple parameters and their interactions [12]. RSM has been successfully applied to the optimization of operational parameters in the modeling of membrane fouling. All proved that RSM is an appropriate and promising tool to optimize a process with one or several responses.

Although RSM is a promising method to address issues related to MF/UF membrane fouling, few works have been done to apply RSM for MF/UF membrane fouling. Accordingly, this study was intended to investigate the influence of process variables such as foulant types (colloidal silica, NOM, and alginate), foulant concentration, and imposed flux on the fouling rate based on RSM. Empirical models were developed to understand the interactive correlation between the responses and process variables.

2. Materials and methods

2.1. Laboratory operation of submerged membrane system

A schematic diagram of the laboratory-scale, submerged hollow fiber membrane system for feed water treatment in this study is shown in Fig. 1. A tank having a working volume of 1 L was used for the filtration test of submerged hollow fiber membrane module. The system consisted of 15 filtration tanks, allowing the simultaneous testing of MF fibers at the same time. Each tank had a working volume of 1 L and a MF fiber was immersed vertically in the reactor. The MF fibers, made of polyvinylidene fluoride (PVDF), were supplied by the LG Electronics, Korea. They have a nominal pore size of 0.2 μm, an internal diameter of 0.7 mm, and an external diameter of 1.3 mm as shown in Table 1. The length of the fiber was 20 cm.

The whole tests were carried out using the same membranes. Permeation from the hollow fiber membrane was pulled by a multi-channel cartridge peristaltic pump (EW-07551-00, Cole-Parmer, USA). The trans membrane pressure (TMP) was continuously measured by a pressure transducer (ISE40A-01-R, SMC, JAPAN) and a data logger (usb-6,008, NI, USA) connected to a computer for data analysis. The temperature of solution was kept constant at 20 °C. A constant flux mode, where both the TMP were increased by foulant deposition and then permeate flux was gradually declined by membrane fouling, was adopted to keep the membrane performance during the operation time.

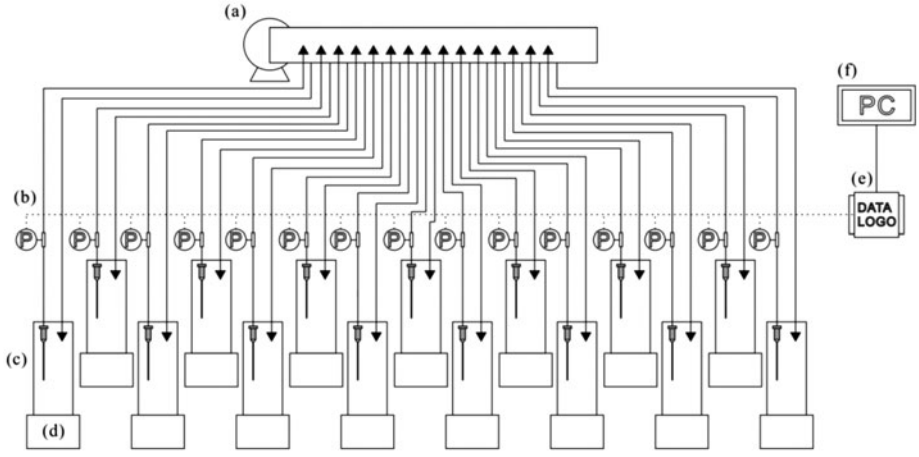

Fig. 1. Schematic diagram of experimental set-up for MF tests; (a) multi-channel peristaltic pump, (b) pressure transducer, (c) hollow fiber, (d) magnet stirrer, (e) data logger, and (f) desktop.

Table 1
Specification of the MF hollow fiber membrane

Module	Submerged module
Filtration method	Dead-end
Flow type	Outside-in
Material type	PVDF/hollow fiber
Length of the module	200 mm
Area of the module	0.01 m^2
Number of fibers	1ea
Pore size	0.2 μm
ID/OD	0.7/1.3 mm

2.2. Preparation of synthetic mixtures

Model foulants used in this study were: kaolin (Sigma Aldrich), silica (Sigma Aldrich, Ludox colloidal silica AM-30), NOM (IHSS, Suwannee river natural organic matter), and alginate (Sigma Aldrich, alginic acid sodium salt from brown algae). Moreover, synthetic feed containing foulants has been employed to investigate the interactions among foulants which cause the membrane fouling. An experimental parameter, including constituent of synthetic feed and adjusted flux, was employed by response surface method as a statistical model. Prior to each filtration test, all membranes were stabilized using deionized water for 120 min.

2.3. Theoretical fundamentals

A simple filtration model was applied to estimate the fouling rates of dead-end microfiltration. Although there are a lot of different fouling mechanisms depending on the characteristics of foulants, pseudo cake filtration model was adopted in this study for simple analysis of data. Based on this model, the permeate flux (J) on the permeate flux at TMP(ΔP) can be described by Darcy's law [13].

$$\Delta P = \eta(R_m + R_c)J \tag{1}$$

where η is the viscosity of water; R_m is the membrane resistance; R_c is the cake resistance; and J is the permeate flux. The cake resistance (R_c) is given by:

$$R_c = \frac{\alpha m_c}{A_m} \tag{2}$$

where α is the specific cake resistance; m_c is the mass of cake deposited on the membrane; and A_m is the membrane area. Here, m_c is proportional to the flux of the foulants:

$$m_c = JA_m c_f t \tag{3}$$

where c_f is the effective foulant concentration. Note that c_f is different from the c_b, which is the bulk concentration of foulant. This implies that all foulants cannot approach the membrane surface due to the back transport. By combining the Eqs. (1–3), ΔP is given by:

$$\Delta P = \eta R_m J + \eta \alpha c_f J^2 t = \eta J R_m + \theta t \tag{4}$$

where θ is the rate of membrane fouling in dead-end filtration tests. Under constant flux conditions, θ can be calculated from the slope of the plot between t and ΔP.

To increase the fouling rate (θ), either J or c_f may be increased. However, θ may not be linearly proportional to J (or c_f). Accordingly, it is important to understand the correlations between θ and J (or c_f), which should be experimentally determined. As indicated in Eq. (4), θ is proportional to J^2. Accordingly, the intrinsic characteristics of foulants, $\eta\alpha c_f$, should be determined by dividing θ by J^2 as a mean of the "normalized" fouling rate, θ/J^2.

2.4. Response surface method

In this study, a statistical model was applied to analyze the fouling on the hollow fiber membranes. The RSM was used to investigate the influence of process variables such as foulant types (kaolin, colloidal silica, NOM, and alginate), foulant concentration, and imposed flux on the fouling rate. The results obtained from the experiments were evaluated by multiple regression analysis method and empirical relationship between the response and independent variables has been expressed by a multi-order polynomial equation. Empirical models were developed to understand the interactive correlation between the responses and process variables.

2.4.1. Experimental design

Based on the results of our preliminary studies, a CCD with four variables and five levels (i.e. −2.0, −1.0, 0, 1.0, and 2.0) was employed. The four independent variables are concentration of kaolin (X_1), concentration of silica (X_2), concentration of NOM (X_3), and concentration of alginate (X_4). The responses are the normalized fouling rate on flux of 80 L/m^2-hr (Y_1) and the normalized fouling rate on flux of 120 L/m^2-hr (Y_2). They can indicate both the fouling phenomenon and the efficiency of the MF process.

The experimental design is shown in Table 2. All experiments were conducted in the order as shown in Table 2.

2.4.2 Statistical analysis and regression analysis

A second order polynomial model, as shown below, was used for regression with the experimental data using Minitab 16.2.0 (Minitab, USA).

$$Y_k = \beta_{k0} + \sum_{i=1}^{4} \beta_{ki} X_i + \sum_{i=1}^{3} \sum_{j=i+1}^{4} \beta_{kij} X_i X_j + \sum_{i=1}^{4} \beta_{kii} X_i^2 \quad (5)$$

where Y_k are the responses, namely Y_1 for the normalized fouling rate on 80 L/m^2-hr, Y_2 for the normalized fouling rate on 120 L/m^2-hr; β_{k0}, β_{ki}, β_{kii}, and β_{kij} are the regression coefficients; and X_i are the coded independent variables. The R^2 and the lack-of-fit are evaluated for fitness of the model.

Table 2
The CCD and the resultant responses

Run	X_1(kaolin)	X_2(silica)	X_3(NOM)	X_4(alginate)
1	−1(5 mg/L)	−1(5 mg/L)	−1(5 mg/L)	−1(5 mg/L)
2	1(15 mg/L)	−1(5 mg/L)	−1(5 mg/L)	−1(5 mg/L)
3	−1(5 mg/L)	1(15 mg/L)	−1(5 mg/L)	−1(5 mg/L)
4	1(15 mg/L)	1(15 mg/L)	−1(5 mg/L)	−1(5 mg/L)
5	−1(5 mg/L)	−1(5 mg/L)	1(15 mg/L)	−1(5 mg/L)
6	1(15 mg/L)	−1(5 mg/L)	1(15 mg/L)	−1(5 mg/L)
7	−1(5 mg/L)	1(15 mg/L)	1(15 mg/L)	−1(5 mg/L)
8	1(15 mg/L)	1(15 mg/L)	1(15 mg/L)	−1(5 mg/L)
9	−1(5 mg/L)	−1(5 mg/L)	−1(5 mg/L)	1(15 mg/L)
10	1(15 mg/L)	−1(5 mg/L)	−1(5 mg/L)	1(15 mg/L)
11	−1(5 mg/L)	1(15 mg/L)	−1(5 mg/L)	1(15 mg/L)
12	1(15 mg/L)	1(15 mg/L)	−1(5 mg/L)	1(15 mg/L)
13	−1(5 mg/L)	−1(5 mg/L)	1(15 mg/L)	1(15 mg/L)
14	1(15 mg/L)	−1(5 mg/L)	1(15 mg/L)	1(15 mg/L)
15	−1(5 mg/L)	1(15 mg/L)	1(15 mg/L)	1(15 mg/L)
16	1(15 mg/L)	1(15 mg/L)	1(15 mg/L)	1(15 mg/L)
17	−2(0 mg/L)	0(10 mg/L)	0(10 mg/L)	0(10 mg/L)
18	2(20 mg/L)	0(10 mg/L)	0(10 mg/L)	0(10 mg/L)
19	0(10 mg/L)	−2(0 mg/L)	0(10 mg/L)	0(10 mg/L)
20	0(10 mg/L)	2(20 mg/L)	0(10 mg/L)	0(10 mg/L)
21	0(10 mg/L)	0(10 mg/L)	−2(0 mg/L)	0(10 mg/L)
22	0(10 mg/L)	0(10 mg/L)	2(20 mg/L)	0(10 mg/L)
23	0(10 mg/L)	0(10 mg/L)	0(10 mg/L)	−2(0 mg/L)
24	0(10 mg/L)	0(10 mg/L)	0(10 mg/L)	2(20 mg/L)
25	0(10 mg/L)	0(10 mg/L)	0(10 mg/L)	0(10 mg/L)
26	0(10 mg/L)	0(10 mg/L)	0(10 mg/L)	0(10 mg/L)
27	0(10 mg/L)	0(10 mg/L)	0(10 mg/L)	0(10 mg/L)
28	0(10 mg/L)	0(10 mg/L)	0(10 mg/L)	0(10 mg/L)
29	0(10 mg/L)	0(10 mg/L)	0(10 mg/L)	0(10 mg/L)
30	0(10 mg/L)	0(10 mg/L)	0(10 mg/L)	0(10 mg/L)
31	0(10 mg/L)	0(10 mg/L)	0(10 mg/L)	0(10 mg/L)

Table 3
Coefficients of the fitted polynomial models for responses

	Y_1 (normalized fouling rate, θ/J^2)		Y_2 (normalized fouling rate, θ/J^2)	
	Coefficient	p-value	Coefficient	p-value
B_0	2.90429	0.000	3.5700	0.001
B_1(X_1, kaolin)	0.25458	0.419	1.3583	0.010
B_{11}	0.15112	0.598	0.5647	0.202
B_2(X_2, silica)	1.04708	0.004	1.1850	0.021
B_{22}	0.73737	0.018	0.3909	0.370
B_3(X_3, NOM)	0.26708	0.397	2.1117	0.000
B_{33}	0.15112	0.598	1.0872	0.021
B_4(X_4, alginate)	1.04792	0.004	1.6645	0.002
B_{44}	0.15237	0.595	−0.2421	0.576
B_{12}	0.20562	0.592	1.0838	0.074
B_{13}	0.00938	0.980	0.5625	0.336
B_{14}	0.00937	0.980	0.8225	0.166
B_{23}	−0.20563	0.592	0.6487	0.269
B_{24}	0.18437	0.630	0.7363	0.212
B_{34}	0.38063	0.326	1.4300	0.023

3. Results and discussion

3.1. Prediction of membrane fouling using the RSM

In the study, the "normalized" fouling rate was used to describe the relationship between concentration of foulants and fluxes. Accordingly, the normalized fouling rate should be controlled by adjusting flux and fouling conditions for constituents of foulants. As an effective statistical tool to predict the effect of foulant concentration and flux, RSM was applied in the study.

Table 4
ANOVA for the polynomial models

Response	Source	Degrees of freedom	Sum of square	F-value	p-value
Y_1	Model	14	76.090	2.41	0.047
	Residual	16	36.1367		
	Lack of fit	10	29.1300	2.49	0.138
	Pure error	6	7.0068		
	R^2	0.6780			
Y_2	Model	14	380.723	5.29	0.001
	Residual	16	82.274		
	Lack of fit	10	65.501	2.34	0.155
	Pure error	6	16.773		
	R^2	0.8223			

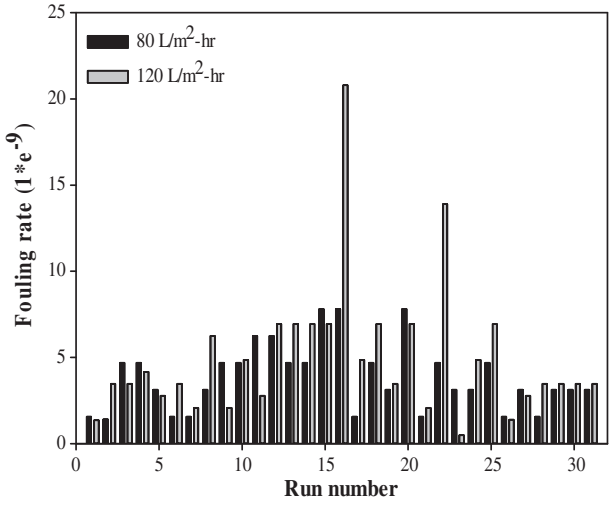

Fig. 2. The resulted responses from the experiments listed in Table 2.

The experimental design and two resulted responses (Y_1 and Y_2) are shown in Table 2. Two second order polynomial regression models were established and tested for adequacy and fitness by the analysis of variance (ANOVA). The regression coefficients (coded factors) of the models for Y_1 and Y_2 are listed in Table 3. The significance of each coefficient was tested by p-value at 0.05, 0.01, and 0.001 levels. All the terms, which are not significant at $p > 0.05$ level, were removed from the models, and the reduced forms of the full polynomial models are as follows:

$$Y_{1,80\ LMH} = 3.29 + 0.25X_1 + 1.05X_2 + 0.27X_3 + 1.05X_4 + 0.7X_2^2 \quad (6)$$

$$Y_{2,120\ LMH} = 4.17 + 1.36X_1 + 1.19X_2 + 2.11X_3 + 1.66X_4 + 1.02X_3^2 + 1.43X_3X_4 \quad (7)$$

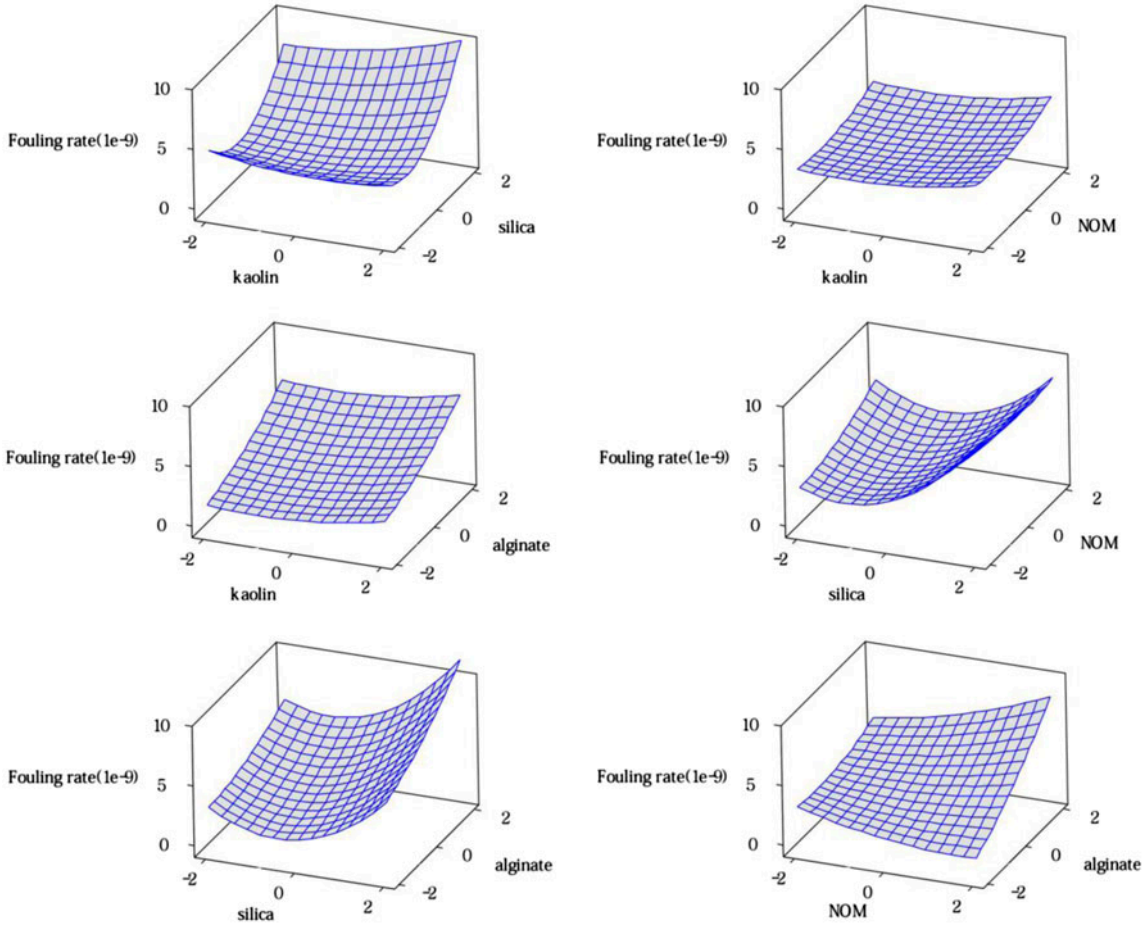

Fig. 3. Response surface of the effects of two independent variables for fouling rate, $Y_{1,80\ LMH}$. The other variable is at zero level in each plot.

where X_1, X_2, X_3, and X_4 take the coded values of the independent variables.

According to the results of ANOVA, the linear terms are all significant for both Y_1 and Y_2, not except the main factor for Y_1 and Y_2; the significant quadratic terms for Y_1 are X_2 and for Y_2 is X_3 only; the interaction terms all are not significant for Y_1, but X_3X_4 are significant for Y_2. The results of ANOVA are shown in Table 4. The R^2s for Y_1 and Y_2 models were 0.6780 and 0.8223, respectively, indicating that the model calculations are reasonable. Moreover, both the lack-of-fits were not significant at $p > 0.05$ level. This indicates that both established models are in good agreement and they are appropriate for representing the relationship between independent variables and responses (Fig. 2).

3.2. Effect and interaction of variables

The effects of the independent variables and their interaction on Y_1 and Y_2 are illustrated as response surfaces in Figs. 3 and 4. As discussed above, kaolin and silica are the most significant factor for fouling rate. As shown in Fig. 3, the normalized fouling rate increases up to 10×10^{-9} for high silica concentrations. This indicates that higher concentration of silica can lead to serious fouling. The fouling rate also increases with increasing alginate concentration. On the other hand, kaolin and NOM show little effect on fouling rate. Accordingly, silica and alginate are more important factors affecting fouling rate than kaolin and NOM at $J = 80\ \mathrm{L/m^2\text{-}hr}$.

As shown in Fig. 4, the effect of kaolin concentration on fouling rate is negligible. However, the kaolin seems to accelerate the fouling by other foulant. This implies that the fouling mechanisms by single compound (colloids or organics) and by two compounds (particles and colloids; particles and organics) are different. Kaolin itself does not significantly cause fouling but it can make fouling by other compound more severe. The statistical analysis based on RSM can help

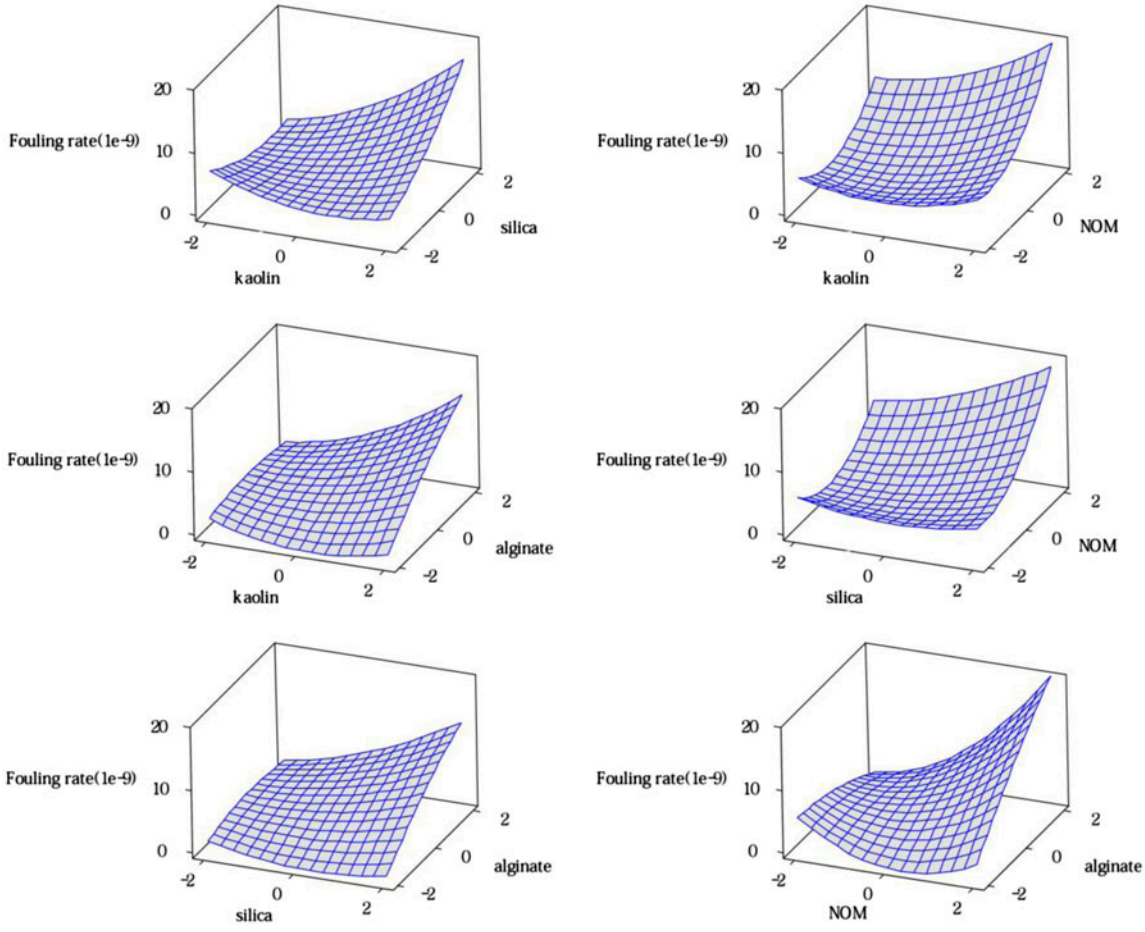

Fig. 4. Response surface of the effects of two independent variables for fouling rate, $Y_{2,120\ LMH}$. The other variable is at zero level in each plot.

to elucidate complex fouling mechanisms by multiple compounds.

The response surface plots for the results at $J = 120\ L/m^2$-hr are shown in Fig. 4. Compared with the results at $J = 80\ L/m^2$-hr, the fouling rate are more strongly dependent on the concentrations of foulants. With an increase in foulant concentrations, the fouling rate becomes higher. It is evident from these response surface plots that there is a synergistic effect of fouling by two foulants. These results are consistent with those reported by previous studies [8].

Interestingly, the major foulants seem to be different at different flux conditions. The combination of silica and alginate lead to the highest fouling rate at $J = 80\ L/m^2$-hr. On the other hand, the combination of NOM and alginate seem to cause the highest fouling rate at $J = 120\ L/m^2$-hr. Since the permeate flux changes the hydrodynamic conditions in membrane filtration, the dominant fouling mechanisms seem to be different depending on the flux. Pore blockage by silica and organic adsorption by alginate appear to be important at $80\ L/m^2$-hr while organic adsorption by NOM and alginate appear to be important at $120\ L/m^2$-hr.

4. Conclusions

In this work, RSM was investigated to analyze fouling propensity of hollow fiber MF membranes. A simple model based on pseudo cake filtration model was applied to estimate the fouling parameters. The model could be successfully applied to interpret experimental data obtained using a laboratory-scale MF system. Although foulant concentration and flux were used to control the rate of fouling, the fouling rate was less sensitive to foulant concentration than to flux. This is because the effective foulant concentration approaching the membrane surface is different from the bulk concentration. RSM was used to examine fouling rate as a function of foulant concentrations in synthetic feed waters. The fouling rates were successfully predicted by the 2nd order polynomial equations. This technique could be also used to investigate the interactions among different foulants, which have various fouling mechanisms. The regression equations from RSM analysis allowed the interpretation of membrane fouling during the filtration of a synthetic feed water containing model foulants. Accordingly, the fouling rate can be easily controlled by adjusting the composition of model foulants and applied flux based on the RSM results, which is essential for the "normalized" fouling rate.

Acknowledgments

This research was supported by LG Electronics, Advanced Research Institute and the National Research Foundation of Korea Grant funded by the Korean Government (MEST), M1A2A2(2010-0029077).

References

[1] L.J. Zeman, A.L. Zydney Marcel Dekker, Microfiltration and Ultrafiltration - Principles and Applications, Wiley, New York, NY, 1996, p. 618.
[2] R.W. Baker, Membrane Technology and Applications, 2nd ed., Wiley, New York, NY, 2004.
[3] P. Weber, R. Knauf, Ultrafiltration of surface water with MOLPURE FW50 hollow fibre module, Desalination 119 (1998) 335–339.
[4] S. Jeong, Y. Choi, T. Nguyen, S. Vigneswaran, T. Hwang, Submerged membrane hybrid systems as pretreatment in seawater reverse osmosis (SWRO): Optimisation and fouling mechanism determination, J. Membr. Sci. 411–412 (2012) 173–181.
[5] T. Lebeau, C. Lelievre, H. Buisson, D. Cleret, L.W. Van der Venter, P. Cote, Immersed membrane filtration for the production of drinking water: Combination with PAC for NOM and SOCs removal, Desalination 117 (1998) 219–231.
[6] A.G. Fane, S. Chang, E. Chardon, Submerged hollow fibre membrane module—Design options and operational considerations, Desalination 146 (2002) 231–236.
[7] D. Mosqueda-Jimenez, R.M. Narbaitz, T. Matsuura, Membrane fouling test: Apparatus evaluation, J. Environ. Eng. 130 (2004) 90–99.
[8] W. Neubrand, S. Vogler, M. Ernst, M. Jekel, Lab and pilot scale investigations on membrane fouling during the ultrafiltration of surface water, Desalination 250(3) (2010) 968–972.
[9] L. Bai, F. Qu, H. Liang, J. Ma, H. Chang, M. Wang, G. Li, Membrane fouling during ultrafiltration (UF) of surface water: Effects of sludge discharge interval (SDI), Desalination 319 (2013) 18–24.
[10] D. Jermann, W. Pronk, R. Kägi, M. Halbeisen, M. Boller, Influence of interactions between NOM and particles on UF fouling mechanisms, Water Res. 42(14) (2008) 3870–3878.
[11] E. Zondervan, B. Roffel, Modeling and optimization of membrane lifetime in dead-end ultra filtration, J. Membr. Sci. 322(1) (2008) 46–51.
[12] R.H. Myers, D.C. Montgomery, Response Surface Methodology: Process and Product Optimization Using Designed Experiments, Wiley, New York, NY, 1995.
[13] H. Darcy, Les fontaines publiques de La Ville Dijon, Victor Dalmont, Paris, 1856.